Research Article | Vol. 25, No. 20 | 2 Oct 2017 | OPTICS EXPRESS 24236
Optics EXPRESS

Laser-writing of ring-shaped waveguides in BGO crystal for telecommunication band

LINGQI LI,[1] WEIJIE NIE,[1] ZIQI LI,[1] CAROLINA ROMERO,[2] RENÉ I. RODRIGUEZ-BELTRÁN,[2] JAVIER R. VÁZQUEZ DE ALDANA,[2] AND FENG CHEN[1,*]

[1]*School of Physics, State Key Laboratory of Crystal Materials, Shandong University, Jinan 250100, China*
[2]*Grupo de Investigación en Aplicaciones del Láser y Fotónica, Departamento de Física Aplicada, University of Salamanca, Salamanca 37008, Spain*
**drfchen@sdu.edu.cn*

Abstract: We report on the fabrication of ring-shaped waveguides operating at the telecommunication band in a cubic $Bi_4Ge_3O_{12}$ (BGO) crystal by using technique of femtosecond laser writing. In the regions of laser written tracks in BGO crystal, positive refractive index is induced, resulting in so-called Type I configuration. The modal profiles are within the designed track cladding with ring-shaped geometries, which are analogous to circular optical lattices. The homogenous guidance along both TE and TM polarizations has been obtained at telecommunication wavelength of 1.55 μm. Both straight and S-curved waveguiding structures have been produced with ring-shaped configurations. This work paves the way to fabricate complex photonic networks for telecommunications by using ring-shaped waveguides in compact chips.

OCIS codes: (230.7370) Waveguides; (140.3390) Laser materials processing; (130.3130) Integrated optics materials.

References and links

1. A. Kumar and S. Aditya, "Performance of S-bends for integrated-optic waveguides," Microw. Opt. Technol. Lett. **19**(4), 289–292 (1998).
2. A. Arriola, S. Gross, N. Jovanovic, N. Charles, P. G. Tuthill, S. M. Olaizola, A. Fuerbach, and M. J. Withford, "Low bend loss waveguides enable compact, efficient 3D photonic chips," Opt. Express **21**(3), 2978–2986 (2013).
3. A. B. Khanikaev, R. Fleury, S. H. Mousavi, and A. Alù, "Topologically robust sound propagation in an angular-momentum-biased graphene-like resonator lattice," Nat. Commun. **6**, 8260 (2015).
4. H.-D. Nguyen, A. Ródenas, J. R. Vázquez de Aldana, J. Martínez, F. Chen, M. Aguiló, M. C. Pujol, and F. Díaz, "Heuristic modelling of laser written mid-infrared $LiNbO_3$ stressed-cladding waveguides," Opt. Express **24**(7), 7777–7791 (2016).
5. W. M. Pätzold, A. Demircan, and U. Morgner, "Low-loss curved waveguides in polymers written with a femtosecond laser," Opt. Express **25**(1), 263–270 (2017).
6. K. T. Koai and P. L. Liu, "Modeling of Ti:$LiNbO_3$ waveguide devices. II. S-shaped channel waveguide bends," J. Lightwave Technol. **7**(7), 1016–1022 (1989).
7. A. M. Kowalevicz, V. Sharma, E. P. Ippen, J. G. Fujimoto, and K. Minoshima, "Three-dimensional photonic devices fabricated in glass by use of a femtosecond laser oscillator," Opt. Lett. **30**(9), 1060–1062 (2005).
8. A. A. Maznev, "Laser-generated surface acoustic waves in a ring-shaped waveguide resonator," Ultrasonics **49**(1), 1–3 (2009).
9. A. Zoubir, C. Lopez, M. Richardson, and K. Richardson, "Femtosecond laser fabrication of tubular waveguides in poly(methyl methacrylate)," Opt. Lett. **29**(16), 1840–1842 (2004).
10. D. Lin and W. A. Clarkson, "End-pumped Nd:YVO_4 laser with reduced thermal lensing via the use of a ring-shaped pump beam," Opt. Lett. **42**(15), 2910–2913 (2017).
11. D. J. Kim, S. H. Noh, S. M. Ahn, and J. W. Kim, "Influence of a ring-shaped pump beam on temperature distribution and thermal lensing in end-pumped solid state lasers," Opt. Express **25**(13), 14668–14675 (2017).
12. K. Sugioka and Y. Cheng, "Ultrafast lasers—reliable tools for advanced materials processing," Light Sci. Appl. **3**(4), e149 (2014).
13. R. R. Gattass and E. Mazur, "Femtosecond laser micromachining in transparent materials," Nat. Photonics **2**(4), 219–225 (2008).
14. S. Antipov, M. Ams, R. J. Williams, E. Magi, M. J. Withford, and A. Fuerbach, "Direct infrared femtosecond laser inscription of chirped fiber Bragg gratings," Opt. Express **24**(1), 30–40 (2016).

#304705 https://doi.org/10.1364/OE.25.024236
Journal © 2017 Received 11 Aug 2017; revised 18 Sep 2017; accepted 18 Sep 2017; published 22 Sep 2017

Optics EXPRESS

15. A. Y. Vorobyev and C. Guo, "Direct femtosecond laser surface nano/microstructuring and its applications," Laser Photonics Rev. **7**(3), 385–407 (2013).
16. K. M. Davis, K. Miura, N. Sugimoto, and K. Hirao, "Writing waveguides in glass with a femtosecond laser," Opt. Lett. **21**(21), 1729–1731 (1996).
17. F. Chen and J. R. Vázquez de Aldana, "Optical waveguides in crystalline dielectric materials produced by femtosecond-laser micromachining," Laser Photonics Rev. **8**(2), 251–275 (2014).
18. Y. Liao, J. Song, E. Li, Y. Luo, Y. Shen, D. Chen, Y. Cheng, Z. Xu, K. Sugioka, and K. Midorikawa, "Rapid prototyping of three-dimensional microfluidic mixers in glass by femtosecond laser direct writing," Lab Chip **12**(4), 746–749 (2012).
19. R. He, I. Hernández-Palmero, C. Romero, J. R. Vázquez de Aldana, and F. Chen, "Three-dimensional dielectric crystalline waveguide beam splitters in mid-infrared band by direct femtosecond laser writing," Opt. Express **22**(25), 31293–31298 (2014).
20. J. Lv, X. Hao, and F. Chen, "Green up-conversion and near-infrared luminescence of femtosecond-laser-written waveguides in Er^{3+}, MgO co-doped nearly stoichiometric $LiNbO_3$ crystal," Opt. Express **24**(22), 25482–25490 (2016).
21. G. Salamu, F. Jipa, M. Zamfirescu, and N. Pavel, "Cladding waveguides realized in Nd:YAG ceramic by direct femtosecond-laser writing with a helical movement technique," Opt. Mater. Express **4**(4), 790–797 (2014).
22. A. Rodenas and A. K. Kar, "High-contrast step-index waveguides in borate nonlinear laser crystals by 3D laser writing," Opt. Express **19**(18), 17820–17833 (2011).
23. R. He, Q. An, J. R. Vázquez de Aldana, Q. Lu, and F. Chen, "Femtosecond-laser micromachined optical waveguides in $Bi_4Ge_3O_{12}$ crystals," Appl. Opt. **52**(16), 3713–3718 (2013).
24. R. Mary, S. J. Beecher, G. Brown, R. R. Thomson, D. Jaque, S. Ohara, and A. K. Kar, "Compact, highly efficient ytterbium doped bismuthate glass waveguide laser," Opt. Lett. **37**(10), 1691–1693 (2012).
25. J. Lv, Y. Cheng, W. Yuan, X. Hao, and F. Chen, "Three-dimensional femtosecond laser fabrication of waveguide beam splitters in $LiNbO_3$ crystal," Opt. Mater. Express **5**(6), 1274–1280 (2015).
26. D. Choudhury, J. R. Macdonald, and A. K. Kar, "Ultrafast laser inscription: perspectives on future integrated applications," Laser Photonics Rev. **8**(6), 827–846 (2014).
27. T. Calmano, A. G. Paschke, S. Müller, C. Kränkel, and G. Huber, "Curved Yb:YAG waveguide lasers, fabricated by femtosecond laser inscription," Opt. Express **21**(21), 25501–25508 (2013).
28. W. Drozdowski, A. J. Wojtowicz, S. M. Kaczmarek, and M. Berkowski, "Scintillation yield of $Bi_4Ge_3O_1$ (BGO) pixel crystals," Physica B **405**(6), 1647–1651 (2010).
29. B. Qian, Y. Liao, G. P. Dong, F. F. Luo, L. B. Su, S. Z. Sun, and J. R. Qiu, "Femtosecond laser-written waveguides in a bismuth germanate single crystal," Chin. Phys. Lett. **26**(7), 070601 (2009).
30. J. Siebenmorgen, K. Petermann, G. Huber, K. Rademaker, S. Nolte, and A. Tünnermann, "Femtosecond laser written stress-induced Nd: $Y_3Al_5O_{12}$ (Nd: YAG) channel waveguide laser," Appl. Phys. B **97**(2), 251–255 (2009).
31. RSoft Design Group, Computer software BeamPROP, http://www.rsoftdesign.com.

1. Introduction

As the basic components in integrated photonics, optical waveguides could confine light propagation within small volumes with dimensions of micrometric or sub-micrometric scales, in which higher optical intra-cavity intensities could be achieved compared with bulk materials. As a result, enhanced optical effects and applications, e.g., lasing and nonlinear responses, could be realized in optical waveguides. In addition, compared with straight waveguide, S-bend waveguides are particularly desirable for the construction of intricate integrated optical waveguide circuits, ideally having minimal bend losses at small curvature radii [1–6].

Ring-shaped waveguides, an essential component of compact and efficient networks of 3D photonic devices in compact chips, have received considerable attention for their diverse application, such as three-waveguide directional couplers, three-dimensional (3D) microring resonators, and surface acoustic wave (SAW) resonators [7–9]. In addition, by using ring-shaped pump beam, a simple approach for alleviating thermal lensing in end pumped solid-state lasers was realized [10,11], which could be also useful to realize efficient waveguide laser systems by ring-shaped wave-guided pump beams. Moreover, ring-shaped waveguides have potential to match the modal profiles of some special fibers (e.g. hollow-core optical fibers) in order to obtain high coupling efficiency. Femtosecond laser writing has been widely applied to implement 3D micro-processing in diverse transparent materials with the excellent advantages for waveguide fabrication since the pioneering work by Davis *et al*. in 1996 [12–16]. The focused femtosecond laser induces localized micro-modification of the materials

Optics EXPRESS

with refractive index changes (negative or positive) through nonlinear absorption processes such as strong-field ionization and avalanche ionization at the focal volume at certain depth [17]. In the low-energy regime, the so-called Type I modification happens, which is correlated to positive changes of the refractive index in the laser-induced tracks [18–22]. In the case of Type II modification, the reduction of refractive index in comparison to the bulk can be observed, which may be caused by lattice expansion in the irradiated region, and the typical strategy is to construct double-line or depressed cladding geometries [23]. Particularly, by using Type I structures it is easier for direct 3D fabrication of complex devices since the guiding cores are located inside the laser-induced tracks. Moreover, Type I waveguides on glass platforms are with well-preserved properties with respect to the bulks, allowing stable and efficient applications for waveguide lasing [24]. Compared with previous simple single line geometry of Type I waveguide [25], the novel configuration in our work shows intriguing modal profiles. The modal profiles are within the designed track cladding with ring-shaped geometries, which are analogous to circular optical lattices. Nevertheless, with limitations in stability and polarization, Type I waveguides have only been reported in a few crystals, including $LiNbO_3$, Nd:YCOB, ZnSe, etc [26]. So far the fabrication of ring-shaped and curved waveguides was mainly demonstrated in glasses, $LiNbO_3$, and Yb:YAG [27].

Bismuth germanate ($Bi_4Ge_3O_{12}$ or BGO) is a well-known scintillating crystal with cubic structure, which has wide applications in nuclear physics, space physics, high-energy physics, medicine, industry and other fields [[28]]. Femtosecond laser writing has been utilized to fabricate straight waveguide in BGO crystal operating in the visible as well as mid-infrared band [[19,29]]. Nevertheless, the guiding properties of Type I waveguides BGO crystal at telecommunication band have not been investigated as of yet.

In this work, we design and fabricate ring-shaped straight and S-curved waveguides based on Type I modification operating at the telecommunication band in BGO crystal by direct femtosecond laser writing. The guiding properties and modal profiles of the waveguides at wavelength of 1.55 μm have been characterized.

2. Experimental details

The cubic BGO crystal sample used in this work was cut into wafers with dimensions of 2 × 10 × 10 mm^3. Figure 1 demonstrates the schematic plot of the direct femtosecond laser writing of ring-shaped waveguides. During the laser writing process, a Ti:Sapphire amplified laser system (Spitfire, Spectra Physics) was utilized, in which linearly polarized pulses (120 fs duration, 796 nm central wavelength, 1 mJ maximum energy, and 1 kHz repetition rate) was generated. The maximum pulse energy on the sample was 4 μJ, and it was controlled by employing a calibrated neutral density filter placed after a half-wave plate and a linear polarizer. The femtosecond laser beam was focused at 150 μm below the largest surface (8 mm × 10 mm) by a 50 × microscope objective with a pulse energy of ~0.11 μJ. During the irradiation, the sample was placed at a 3D motorized stage with a spatial resolution of 0.2 μm and was scanned at a constant velocity of 500 μm/s in the direction perpendicular to the laser polarization and the pulse propagation. The scanning direction was carefully aligned with the 10-mm edge, thus performing a damage line inside the sample. The procedure was repeated and several parallel tracks (3 μm lateral separation of adjacent parallel tracks) were written at different depth forming the desired circular geometry of the cladding. Four types of waveguides with straight, and S-curved with lateral offset 50, 100, and 150 μm have been fabricated by this procedure. Under the same laser irradiation parameters, we fabricated waveguides with two ring diameters of 50 μm and 100 μm.

After laser writing, the end faces were optically polished for measuring the guiding properties of the waveguides, resulting in a final length of 9.9 mm for all the waveguides. The cross-sectional microscope images of ridge waveguides were taken by using an optical microscope (Axio Imager, Carl Zeiss) operating in transmission mode. The near-field modal

Optics EXPRESS

profiles were investigated by employing a typical end-face arrangement. A 1.55 μm fiber laser was employed and the Glan-Tayler prism was used to control the polarization. The laser was then coupled into the end-face of the BGO sample by an objective lens (N.A. = 0.40). Afterwards, the modal profile at the output of the waveguide was imaged by CCD by another same objective lens. The coupling beam size was same for waveguides with diameter of 50 μm and 100μm. Based on the above arrangement, the propagation losses were determined by directly measuring the light powers coupled into and out of the end-faces, taking the coupling and Fresnel reflection losses of the waveguide systems into account as well.

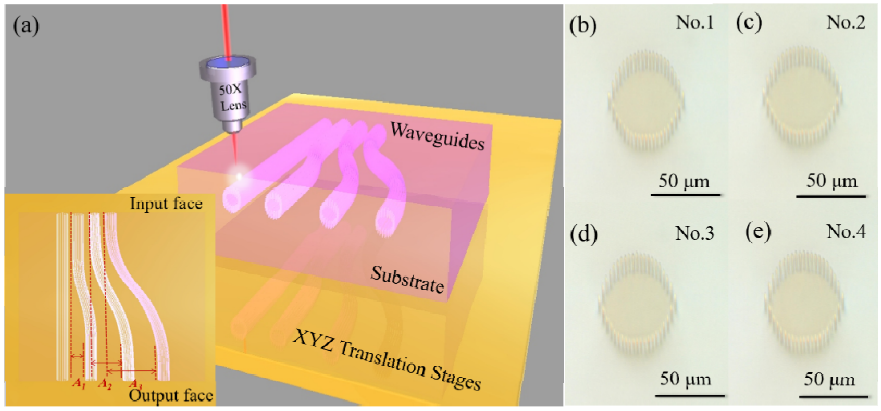

Fig. 1. The fabrication of straight and S-curved waveguides in BGO. (a) Schematic plot of the fabrication process with the femtosecond laser. The inset picture is the schematic diagram of S-curved waveguides. L denotes the lateral offset of S-curved waveguides, A_1 (50 μm), A_2 (100 μm) and A_3 (150 μm), respectively. Optical microscope image of the cross section of waveguides (b) No. 1. straight, (c) No. 2. A_1 = 50 μm, (d) No. 3. A_2 = 100 μm, and (e) No. 4. A_3 = 150 μm.

3. Results and discussion

The general shape of straight and S-curved waveguides considered has been shown in the inset picture of Fig. 1(a), with the lateral offset A between the input and output ports. Three types of S-curved waveguides were designed with lateral offset values of 50 μm (A_1), 100 μm (A_2), and 150 μm (A_3). Figures 1(b)-1(e) exhibit the 50-μm-diameter circular cross-sectional microscope images of waveguides Nos. 1-4, corresponding to waveguide of straight and S-curved A_1, A_2 and A_3, respectively. Different from the depressed cladding waveguide core located in the regions surrounded by the laser inscribed tracks, the waveguide core of this structure was located in circular regions constructed by femtosecond laser written tracks. The S-curved waveguides parameterized with a $\sin^2\theta$ function with the Eq. (1)

$$y(x) = A\sin^2(\frac{\pi x}{2L}) \quad (1)$$

where L is the length of the crystal and the parameter A is the lateral offset between the input and output ports. Figures 2(a)-2(d) depict the measured near-field modal profiles of waveguides Nos. 1-4 along both the TE and TM polarizations at wavelength of 1.55 μm. Generally, Type I waveguides in crystals reported before mainly support guidance along one particular polarization [21,22]. This profile was characteristic of a ring-shaped waveguide, in which guiding occurs within an annular core. The intriguing modal profiles were analogous to circular lattice geometry, which could be designed with the required diameter to meet the practical applications. As expected, the similar modal profiles were also found in the waveguides Nos. 5-8 with diameter of 100 μm as shown in Figs. 2(e)-2(h).

Optics EXPRESS

In order to reconstruct the profile of the increased refractive index in the modified regions, we used the technique developed by Siebenmorgen *et al* [30]. The calculated maximum refractive index contrast was estimated to be $(5.0 \pm 1) \times 10^{-3}$ for BGO waveguides at 1.55 μm. Fig. 3 shows the simulated the light propagation and mode profiles at 1.55 μm by using the commercial program BeamPROP (Rsoft, Inc), which is based on the finite-difference beam propagation method (FD-BPM) [31]. To determine more accurately the magnitude of the refractive index change (Δn), the same waveguide design was tested in the software with different values of Δn, ranging from 4.0×10^{-3} to 6.0×10^{-3} in 0.1×10 steps. By comparing the simulated profiles with the measured near-field intensity distributions in Fig. 3, the refractive index changes of the waveguide were determined to be 4.8×10^{-3}, for which the best agreement with the experimental results was obtained.

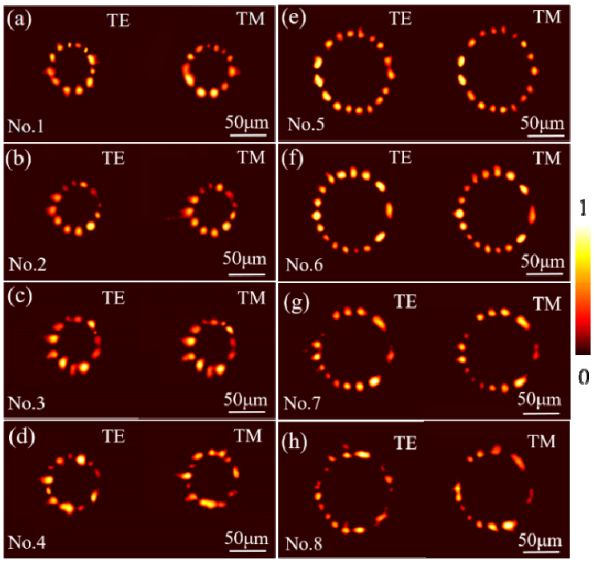

Fig. 2. Measured near-field modal profiles of waveguides Nos.1-4 (diameters of 50 μm) and Nos. 5-8 (diameters of 100 μm) for TE (left) and TM (right) polarizations at 1550 nm, respectively.

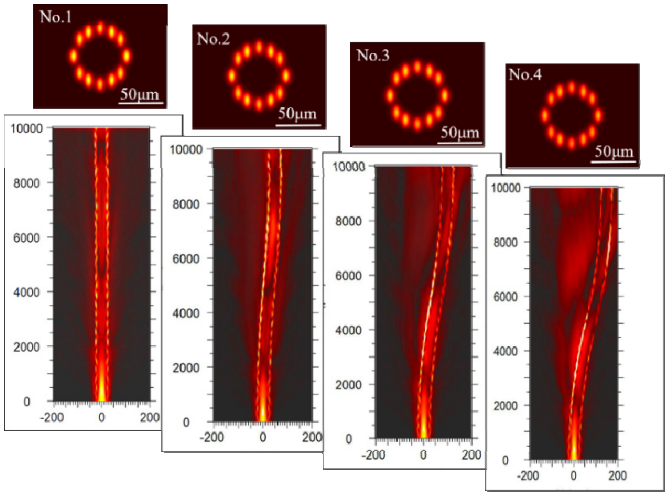

Fig. 3. Simulated mode profiles and beam propagation at 1.55-μm in straight and S-curved waveguides with different lateral offset *A* arranging from 50 μm to 150 μm.

Optics EXPRESS

Table 1. Propagation losses α (dB/cm) of BGO straight and S-curved waveguides

	No.1	No.2	No.3	No.4	No.5	No.6	No.7	No.8
TM	1.56	1.88	2.18	2.31	0.98	1.27	1.61	1.72
TE	1.63	1.91	2.17	2.35	1.03	1.24	1.56	1.67

Table 1 shows the propagation losses (α) of the laser-written straight and S-curved waveguides. As one can see, the differences between TE and TM polarizations were less than 7%, showing the good features of polarization-insensitive guidance. In order to thoroughly investigate the polarization properties of the waveguides, the all-angle light transmission of the guidance was shown in Fig. 4. It is found that the guidance exists for the 1.55 μm laser light at any polarizations. To create compact and efficient networks of photonic structures, not only low propagation losses but also reasonable bend losses are required which depend upon a large positive index contrast Δn. By comparing the propagation losses of the straight and S-curved waveguide written with the same parameters, the bend losses of the different lateral offset have been estimated. The bend losses of S-curved waveguide with diameter 50 μm along TE polarizations were 0.28, 0.54, 0.72 dB for lateral offset of 50, 100 and 150 μm, respectively. In addition, the values of bend losses of S-curved waveguide with diameter 100 μm were 0.21, 0.53 and 0.64 dB for lateral offset of 50, 100 and 150 μm, respectively. As one can see, the bend loss increases with the increase of the lateral offset of S-curved waveguides from 50 to 150 μm. Otherwise, it can be clearly seen that the largest bend losses from the lateral offset A = 150 μm of the S-curved waveguides is determined to be less than ~0.75 dB, which exhibit the superb potentiality applied in compact chips.

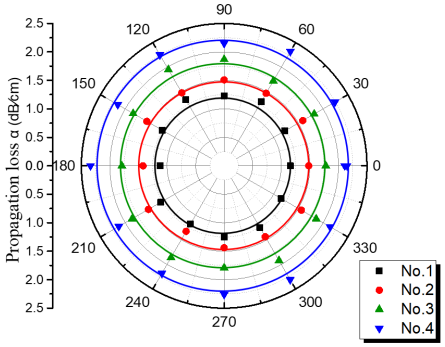

Fig. 4. Polarization images of the propagation loss of waveguides Nos. 1-4 at 1.55 μm.

4. Summary

In conclusion, we have demonstrated the design and fabrication of ring-shaped straight and S-curved waveguides in BGO crystal by direct femtosecond laser writing of Type I index modification. These waveguides exhibit intriguing modal profiles, which are analogous to circular lattice geometry along both the TE and TM polarizations at telecommunication wavelength of 1.55 μm. The waveguides have low propagation losses at 1.55 μm. In addition, the S-curved waveguides show no significant bending losses, which could be used to construct compact and efficient networks of 3D photonic structures. Moreover, this waveguide configuration by laser writing may also be implemented in other optical crystals to achieve diverse applications.

Funding

Natural National Science Foundation of China (NSFC) (61775120); Junta de Castilla y León (Project SA046U16); Spanish Ministerio de Economía y Competitividad (MINECO, FIS2013-44174-P, FIS2015-71933-REDT).